

PROGRESS ON THE NEW HIGH GRADIENT C BAND STANDING WAVE RF PHOTO-GUN

D. Alesini, F. Cardelli, G. Di Raddo, L. Faillace, M. Ferrario, A. Gallo, A. Giribono, A. Gizzi, S. Lauciani, A. Liedl, V. Lollo, L. Pellegrino, L. Piersanti, C. Vaccarezza and A. Vannozzi, INFN-LNF, Frascati, Italy. L. Ficcadenti, INFN Roma, Italy.

Abstract

The new C-Band RF gun, developed in the context of the European I.FAST and INFN Commission V projects, has been realized. It is a 2.6 cell standing wave cavity with a four-port mode launcher, designed to operate with short rf pulses (300 ns) and cathode peak field larger than 160 MV/m. The gun has been realized with the new technology without brazing, developed at INFN, that allows to assemble the gun cells with special gaskets and to proceed, after the vacuum test, directly to the rf characterization. In the paper we illustrate the realization procedure and the results of the vacuum and low power RF tests. The gun is now ready for the final setup phase with the implementation of the cooling distribution system that will allow the high power test at PSI (Switzerland).

INTRODUCTION

The realization and test of a C Band photo-gun has been funded by the EU in the framework of the I.FAST project [1] and by INFN Commission V. The possibility to implement a full C-band injector is strongly attractive for both the reachable beam parameters [2] and compactness than for the possibility to operate at high repetition rate (up to 1 kHz), especially in the context of the X-band linacs of the EuPRAXIA@SPARC_LAB project [3] and XLS design study [4]. The gun is also extremely attractive for its possible applications in upgrades of existing photo-injectors for FEL. The electromagnetic and thermo-mechanical analysis have been already illustrated in previous papers [5] and the main parameters are reported in Table 1.

Table 1: Main Parameters of the C-band Gun (in parenthesis the measured ones)

Parameter	Value
Resonant frequency	5.712 (5.712)
$E_{\text{cath}}/\sqrt{P_{\text{diss}}}$ [MV/(m·MW ^{0.5})]	51.4
rf input power [MW]	18(19)
Cathode peak field [MV/m]	160
Rep. rate [Hz]	100-400
Quality factor	11900 (11900)
Filling time [ns]	166 (147)
Coupling coefficient	3 (3.5)
rf pulse length [ns]	300
Mode sep. π - $\pi/2$ [MHz]	47 (48.3)
$E_{\text{surf}}/E_{\text{cath}}$	0.96
Mod. Poy. vector [W/ μm^2]	2.5
Pulsed heating [°C]	16
Average diss. Power [W]	250-1000

The 3D mechanical layout of the whole injector is given in Fig. 1. The gun is followed by an emittance compensating solenoid and a laser injection chamber that allows the laser injection with the last mirror in air. The gun has been realized without brazing, with the new technology developed at INFN and already adopted for the realization of RF photo-guns in S band [6,7]. The technology allows to assemble the gun with special gaskets in a clean room and to proceed, after the vacuum test, directly to the rf characterization. The main advantage is the possibility to use forged, not annealed, copper that, according to X band high gradient tests [8] and our tests on S band gun [6,7] has been verified to exhibit extremely good performances in term of conditioning time and breakdown rate. In the present paper we illustrate the gun realization procedure and the low power rf measurements results on the final gun. We also briefly introduce the new feeding scheme we have proposed to power the gun without isolator.

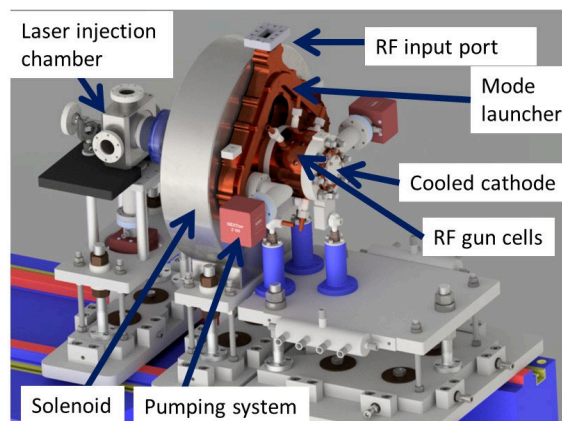


Figure 1: 3D Mechanical Layout of The Gun.

GUN COMPONENTS FABRICATION AND ASSEMBLY

The gun integrates several different components: the standing wave (SW) cells, the four-port mode launcher and the cathode. The mode launcher has been machined using the five-axis milling machine Micron UCP600 Vario with precision on the internal dimensions of $\pm 8 \mu\text{m}$ and roughness below 200 nm. It has then been brazed in a vacuum furnace using palcusil 5 alloy. Pictures of the machined mode launcher before and after brazing are given in Fig. 2. After brazing it has been vacuum tested. RF tests have been also performed, mounting the aluminum cells used for the previously fabricated prototype [5]. The SW cells and cathode have been machined using, for the final finishing of the surfaces the lathe Schaublin 225 TM-CNC. Pictures of the machined cells before the final assembly are reported in Fig. 3. The internal dimensions of the cells have

been machined with a precision of $\pm 2 \mu\text{m}$ and a surface roughness below 30 nm. After the machining, the cells have been cleaned using a bath of Almeco, followed by an NGL cleaning at 50 °C and a final treatment in citric acid at 40 deg to remove the oxidations. They have been finally washed with demineralized water in an ultrasonic bath and dried with pure nitrogen. After the cleaning the cells have been also heated in a vacuum furnace at 200 °C for 2 hours to remove the residual water from the surfaces.

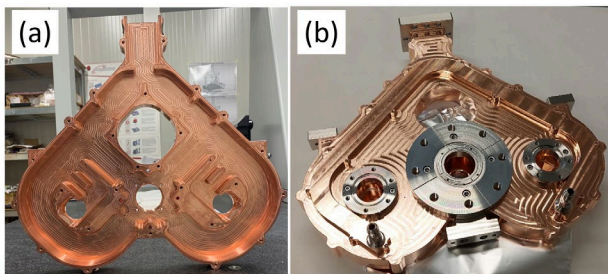


Figure 2: Pictures of The Machined Mode Launcher Before (a) and After Brazing (b).

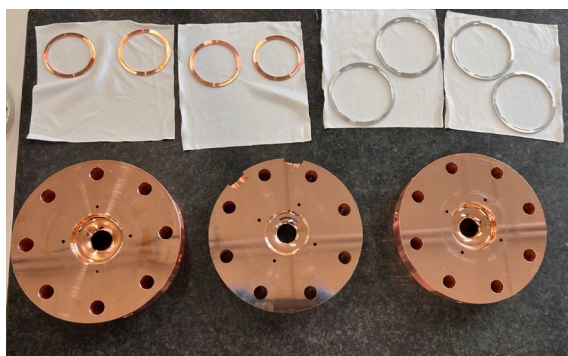


Figure 3: Pictures of The SW Copper Cells.

The gun has been finally assembled. The mounting procedure of the cells on the gun is illustrated in Fig. 4. In all the mounting procedure the gun has been flushed with dry nitrogen. The mounting procedure foresaw the use of two special gaskets. The external one, in aluminum for vacuum seal and the internal one with a special copper gasket for the rf contact. The alignment of the cells has been guaranteed, during the mounting procedure, using two special “V” precise tools has shown in Fig. 4(c). The gun, after the final assembly, has been vacuum tested with leak rate sensitivity below 1×10^{-11} mbar/l/s. The picture of the final assembled gun under vacuum tests is given in Fig. 4(d). The assembled gun has been mechanically characterized, after the final assembly, using a CMM ALTERA 10.7.7 (Fig. 5b) and the alignment of the cells has been verified to be, in both planes, below $\pm 40 \mu\text{m}$.

RF GUN TEST RESULTS

The assembled gun has been RF tested using a Network Analyzer R&S ZVB 20 (Fig. 5(a)). The measurements have been done under nitrogen flux. The reflection coefficient at the input port is reported in Fig. 6. The three modes are clearly visible in the plot. The frequency of

operation, quality factor and coupling coefficient obtained by fitting the reflection coefficient are reported in Table 1. They clearly show that the frequency and quality factor of the working mode are the nominal ones while the coupling coefficient is slightly larger. The reasons of this discrepancy are still under investigation and are probably related to the different dimensions of the first coupling iris. This value of the coupling coefficient does not affect significantly the gun performances in term of required power, rf pulse length and cathode peak field. The electric field on axis has been measured using a metallic bead of 2 mm diameter connected to a nylon wire, dropping into the gun. The result of this measurement is reported in Fig. 7. The field unbalance between the cells is at the level of 5%. With the bead drop technique it is not possible to measure the cathode peak field at the cathode plane because of the effects of image currents that affect the measurement itself. The field at the cathode position, extrapolated by a local fit of the measurements, has a value comparable with the field on the first cell, 5% below the central one. The reason of this discrepancy with respect to the ideal simulated value are still under investigation and are probably due to the small deformation of the special copper gaskets used to guarantee the rf contact and tolerances in the fabrication that, even if at the level of few μm , can still affect the field flatness.

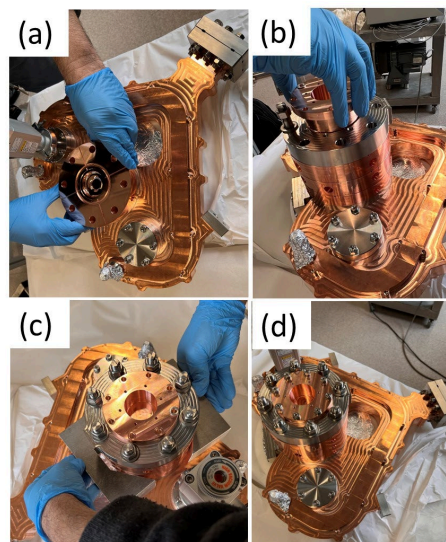


Figure 4: Pictures of The Gun Under Assembly: (A) Assembly of The Cells; (B) Cathode Insertion; (C) Cell Alignment Before the Final Clamping; (D) Vacuum Test;



Figure 5: (a) RF Tests of The Gun; (b) Mechanical Characterization of the Gun With CMC.

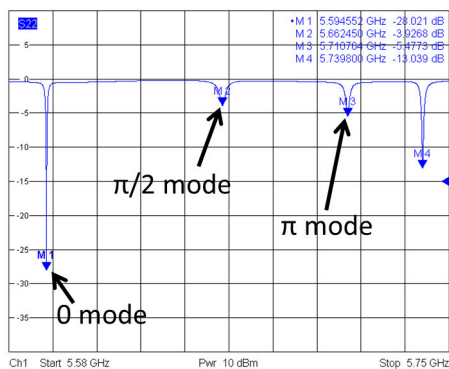


Figure 6: Reflection Coefficient at The Gun Input Port

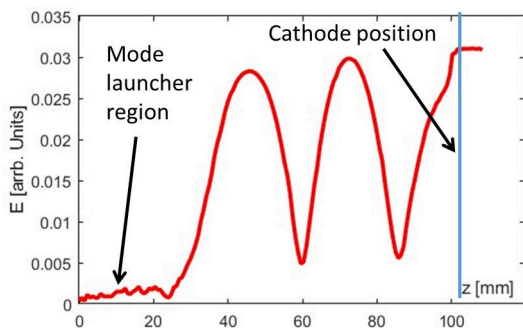


Figure 7: Electric Field Profile on Axis Measured by Bead Drop Technique

GUN FEEDING SCHEME WITHOUT ISOLATOR

The original gun feeding scheme foresaw the use of a new in-vacuum isolator. The delivery of the isolator experienced some delays due to the difficulties that have been encountered in its realization. For this reason and also to have a backup solution in case of difficulties in reaching, with this new device, the required performances in term of power, we have developed an alternative scheme using power dividers and a BOC-type pulse compressor already available at PSI for the test of the travelling wave gun in the context of the I.FAST project [1]. The scheme is represented in Fig. 8. The power from the klystron is splitted with a ratio 1:10 with a power splitter and is then compressed with the pulse compressor. The reflected power from the cavity is splitted back with the same ratio. The calculated input power into the gun and the cathode peak field are reported in Fig. 9 while the reflected power to the klystron does not exceed the 500 kW level, as reported in Fig. 9(c). In all the calculations we have considered a 10% waveguide attenuation and rise/decay times of the phase switch and rf pulse of 150 ns. The scheme allows to reach the 160 MV/m cathode peak field and, even if the isolator will be finally available for the high power test, it will be implemented since represents an interesting and alternative feeding scheme for high power SW structures.

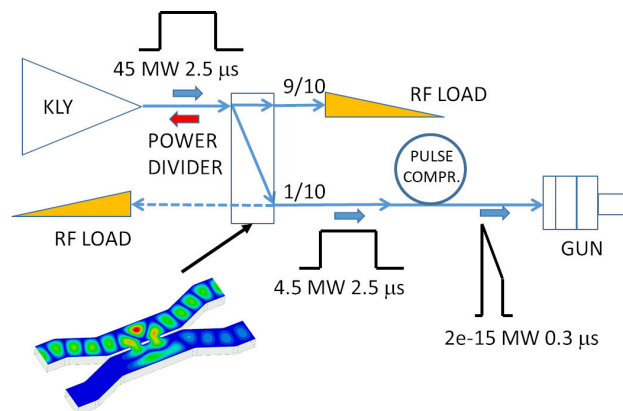


Figure 8: Alternative Gun Feeding Scheme w/o Isolator

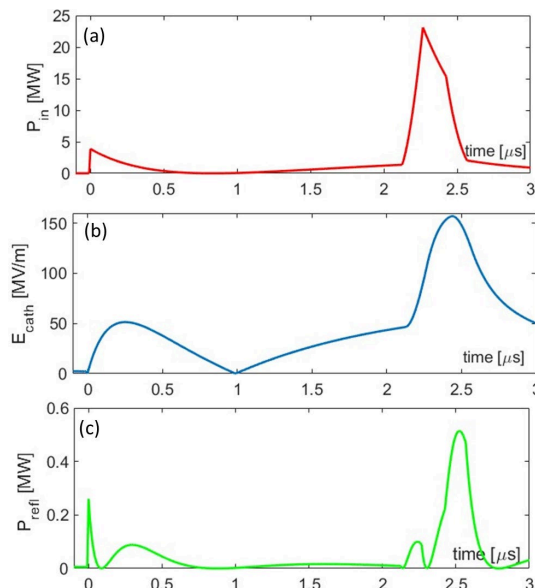


Figure 9: (a) Calculated Input Power To The Gun With Alternative Feeding Scheme; (b) Cathode Peak Field; (c) Reflected Power To The Klystron

CONCLUSIONS

The new SW C band gun has been fabricated with the new technology without brazing and has been vacuum and rf tested. The rf parameters are in quite good agreement with expectations and the gun is now ready to be integrated in the setup for the high power test to be done at PSI in the context of the I.FAST project. A new feeding scheme without the use of the isolator has been also proposed and will be implemented in parallel with the original scheme.

ACKNOWLEDGEMENTS

We would like to acknowledge the COMEB Company [9] for the technical support in gun realization. This project has received funding from the European Union's Horizon 2020 Research and Innovation program under GA No101004730 and from the INFN Commission V.

REFERENCES

- [1] CERN, <https://ifast-project.eu/home>
- [2] A. Giribono et al., “Generation of high brightness electron beam in a normal conducting - high repetition rate C-band injector”, unpublished.
- [3] M. Ferrario et al., “EuPRAXIA@SPARC_LAB “Design study towards a compact FEL facility at LNF”, arXiv:1801.08717.
- [4] Compact, <http://www.compactlight.eu/Main/HomePage>
- [5] D. Alesini et al., “The new c band gun for the next generation rf photo-injectors”, in Proc. IPAC'22, Bangkok, Thailand, Jun. 2022, pp. 679-682.
doi:10.18429/JACoW-IPAC2022-MOPOMS021.
- [6] V. Shpakov et al., “Design, optimization and experimental characterization of RF injectors for high brightness electron beams and plasma acceleration,” J. Instrum., vol. 17, no. 12, p. P12022, Dec. 2022,
doi: 10.1088/1748-0221/17/12/p12022.
- [7] D. Alesini et al., “Design, realization, and high power test of high gradient, high repetition rate brazing-free S-band photogun”, Phys. Rev. Accel. Beams vol. 21, no. 11, Nov. 2018, doi:10.1103/physrevaccelbeams.21.112001.
- [8] E. I. Simakov, V. A. Dolgashev, and S. G. Tantawi, “Advances in high gradient normal conducting accelerator structures,” Nucl. Instrum. Methods Phys. Res., Sect. A, vol. 907, pp. 221–230, Nov. 2018,
doi: 10.1016/j.nima.2018.02.085.
- [9] COMEB, <http://www.comeb.it/>.